General Introduction and Objectives of the Thesis Work

1. General Introduction

The introductory chapter commences the basic insights about the limited reserve and climatical impact of fossil fuels, the importance of alternatives to fossil fuel energy sources, energy converting and storage devices, especially regenerative fuel cells (FCs), metal-air batteries (MABs) etc. The principles of FC (particularly polymer electrolyte membrane fuel cells (PEMFCs)) and MAB, the types of reactions involved, and current challenges have been discussed. The oxygen reduction reaction (ORR) and oxygen evolution reaction (OER) being the prime reactions in PEMFCs and MABs are extensively emphasized in this chapter. In continuation, a brief literature review on the designing of noble metal-based and noble metal-free electrocatalysts (ECs) along with their potential advantages and disadvantages are included. This chapter also includes an extensive literature survey related to different types of metal oxides (MOs) as ORR/OER ECs and the role of carbon support on which the final objectives for the present investigation are established.

1.1. Overview

Green energy and the search for alternatives to conventional energy sources has been the area of extensive research over the last century. With the exponential growth of population and depletion of conventional energy sources (oil, natural gas, coal, etc.), the energy crisis seems to be inevitable soon. Additionally, the adverse environmental impact of the greenhouse gases (GHGs) produced by the massive combustion of fossil fuels, has also become a major concern [1–4]. The steep increase in the GHGs have been triggering global warming and facilitating inexplicable climate changes [5–7]. Figure 1(a, b) displays the annual global energy consumption (EJ) from the fossil fuel sources along with the fossil, chemical industry and flair CO_2 emissions during the last two decades. In the global energy consumption scenario, BPs (British Petroleum) 'Statistical Review of World Energy 2020' which reported a comprehensive picture of supply and demand for major energy sources on a country-level basis, has revealed that fossil fuels still contribute 84% of global energy demands [8]. Simultaneously,

with the massive deployment of fossil fuels, a huge amount of CO_2 emissions is inevitable. A statistical report on global CO_2 emissions reveals that about 89% of CO_2 emissions in 2018 originated from fossil fuels and the chemical industry [9]. However, from 2019 to date a substantial decline in both global energy demand and global CO_2 emissions might be noticeable which is attributable to COVID-19. As a consequence of the current critical energy and environment situation, it is now indispensable to accelerate the movement to get off fossil fuels exploring potential alternative energy sources to mitigate the energy crisis in a greener way. Stepping towards the ambition to accomplish sustainable and readily accessible power sources, the global scientific community have been concentrating their work on various renewable alternative energy resources such as solar, hydrogen, biomass, waves, tides, wind, rain, geothermal, nuclear power, etc. [10–13]. In recent times, hydrogen (which involves the use of hydrogen and/or hydrogen-containing compounds), oxygen and solar energy, being clean and carbon-free, is well-recognized as a potential renewable energy source [11,12,14].

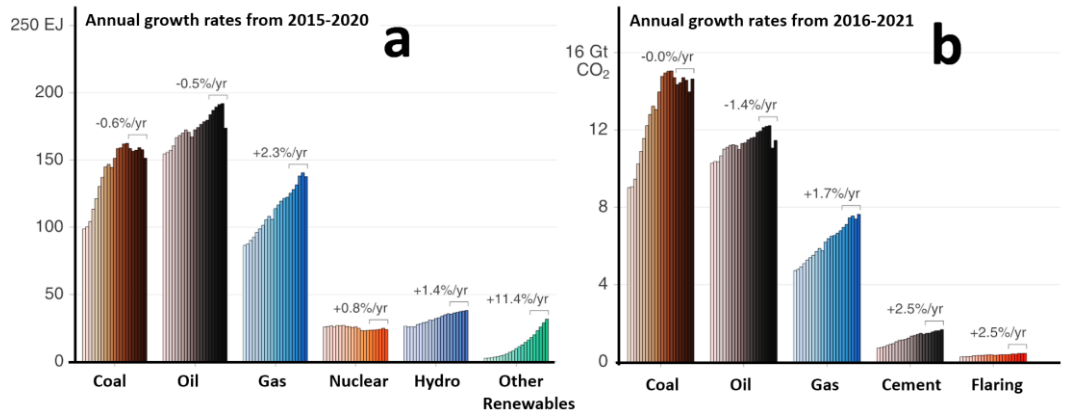

Figure 1.1 a) Annual global energy consumption (EJ) by fuel source from 2000 through 2020 with average annual growth rates for each fuel shown under brackets for the period 2015 through 2020; b) Fossil CO_2 emissions by fuel type (coal, oil, and natural gas) plus emissions from cement production and flaring; note that these emission estimates do not include methane leakage during extraction and use. Average annual growth rates for each fuel are shown under brackets for the period 2016 through 2021. (Adapted with permission from [15]).

Consequently, solar cells, the FCs and MABs have attracted growing interest in recent times primarily because of their independence from fossil fuels [11,16,17]. Additionally, the direct transformation of chemical to electrical energy is much more efficient as it steps aside the entropy consequences that are common in converting heat into mechanical work. Thus, it is now clear and widely considered that the FCs and MABs have become indispensable components participating in the movement to get off fossil fuels which are potential alternative energy technology for the clean energy revolution.

1.2. Fuel Cells and Metal-Air Batteries

The chemical energy reserved in fuels can be directly converted to suitable electrical energy through the electrochemical devices such as FCs, MABs, etc. [18,19]. Unlike conventional combustion engines, FCs and MABs batteries do not have multiple mechanical steps in the process of energy transformation as they are not associated with burning of the fuel and run pistons or shafts. A schematic of energy conversion steps that involve in a conventional heat engine and FC is shown in Figure 1.2. As a consequence of the single-step mechanism FCs and MABs extend the scope of highly efficient energy conversion with significantly low emissions and environmentally safe operating conditions. The power generated from FCs and MABs

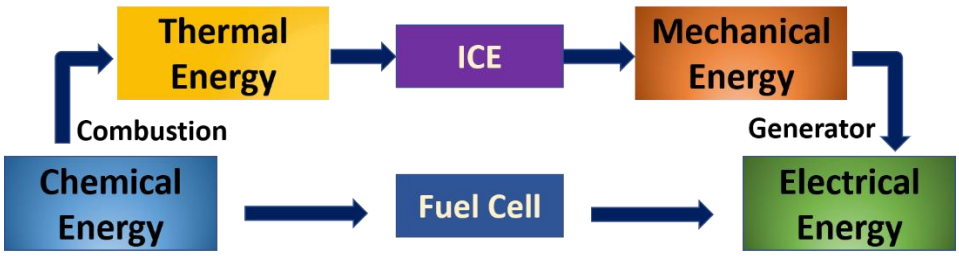

Figure 1.2: Electricity generation process steps involved in a conventional internal combustion engine (ICE) and FCs.

can be utilized in a broad area of application across numerous sectors, including transportation, industrial, commercial, and residential buildings, and long-term energy storage for the grid in reversible systems. FCs are characterized into several types based on the electrolytes employed. Hydrogen-based FCs produce only water as a bi-

product, addressing the normalization of the critical climate challenges as it offers carbon-free emissions. Moreover, they produce no significant sound pollution during operation as they have fewer moving parts. Different types of FCs along with their operating temperature and characteristics components are shown in Figure 1.3. Among these, polymer electrolyte membrane fuel cells (PEMFCs) are observed to be a greener, futuristic and potential technology as the electrical power generator, since they can be operated at the convenient temperature (<100 °C) and develops broader attention because if its high energy density, high energy conversion efficiency and environment-friendly nature, which further extends usable flexibility in multiple applications [20,21]. A unitized regenerative proton exchange membrane fuel cell (URPEMFC) is another class of energy-converting electrochemical appliance that can operate both as an electrolyser and a FC. The working mode of the device can be switched from electrolyser to FC and vice versa whenever it is needed [22].

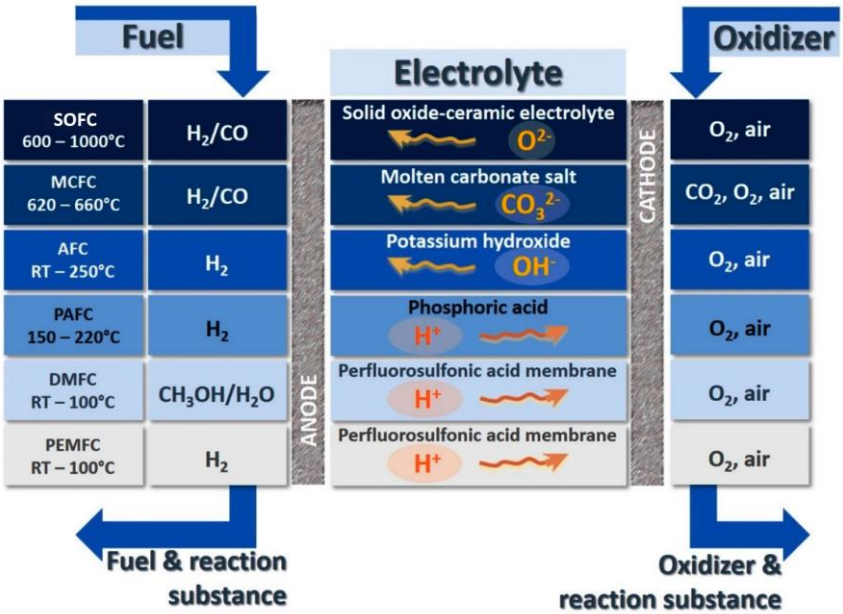

Figure 1.3. Overview of different types of FCs (SOFC- solid-oxide fuel cell, MCFC- molten carbonate fuel cell, AFC- alkaline fuel cell, PAFC- phosphoric acid fuel cell, DMFC- direct methanol fuel cell, PEMFC- polymer electrolyte fuel cell) with its basic components and operational temperature. (Adapted with permission from [23]).

1.2.1. Principles of PEMFCs

PEMFC is primarily a device with a multi-layered assembly comprising of a polymer electrolyte membrane, sandwiched between a gas diffusion layer (GDL), electrode and electrode-catalyst (currently Pt and Pt-based material) [24,25]. A typical schematic diagram of PEMFC with the membrane electrode assembly and other various functional components is presented in Figure 1.4. Usually, per-fluorosulfonic acid (PFSA) membranes such as Dupont's Nafion® with per-fluorinated backbones and sulfonic acid as the terminal group, is the widely used as polymer electrolyte

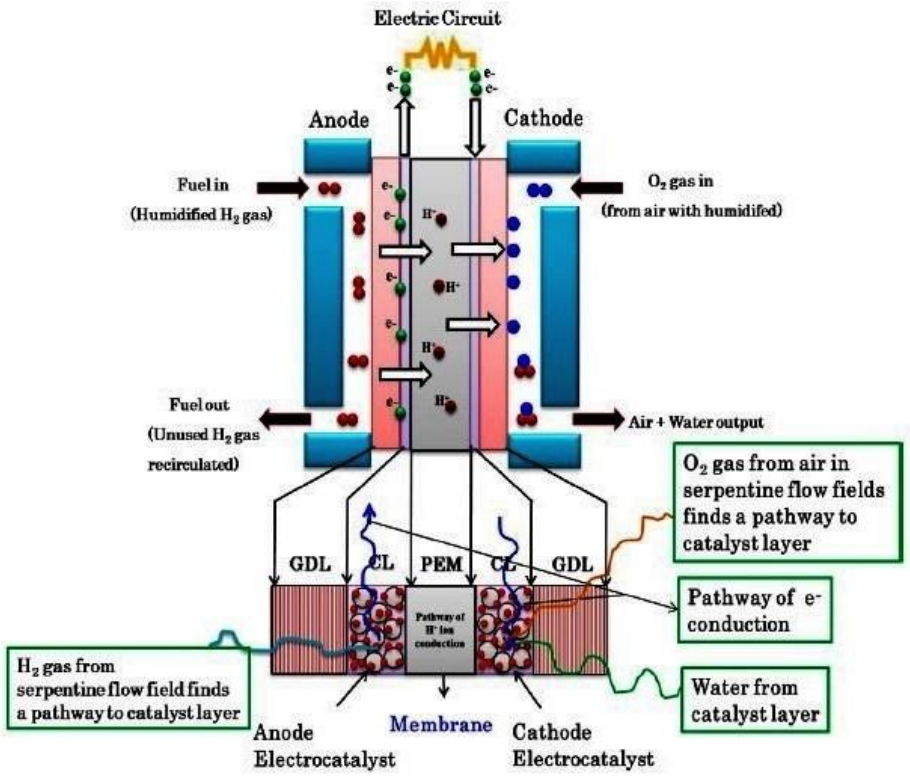

Figure 1.4 Schematic of the membrane electrode assembly with other functional components PEMFC.(Adapted with permission from [25]).

membrane (PEM) in PEMFCs for decades, owing to their excellent working performance and long durability [26]. PEM can act as an electronic insulator and reactant barrier between the electrodes, while it plays the key role of transporting H^+ ions from the anode to the cathode of the PEMFC. In principle, the H_2 is activated at the anode and forms the H^+ and e^-. The H^+ ions move from the anode to the cathode

through the PEM and the e^- (s) transport through the external circuit to the cathode followed by electrocatalytic reduction of the O_2. Eventually, the H^+ ions released from the anode, passing through the PEM, encounter the reduced oxygen species producing heat and water [24,25]. The cathodic reaction in PEMFCs is essentially the ORR. Notably, the overall efficiency of the device is controlled by ORR. The reactions involved in PEMFCs are

At anode:	$H_2\,(g) \rightarrow 2H^+\,(aq) + 2e^-$	(1.1)
At cathode:	$½\,O_2\,(g) + 2H^+\,(aq) + 2e^- \rightarrow H_2O\,(l)$	(1.2)
Overall reaction:	$H_2\,(g) + ½\,O_2(g) \rightarrow H_2O\,(l)$	(1.3)

1.2.2. Principles of MABs

The fundamental working principle of both FC and MAB devices is rather similar. The basic components of a MAB include a metal electrode (anode), an air electrode (cathode) and an aqueous or non-aqueous based electrolyte. For anode material, normally metal species such as Zn, Al, Li, Na, Mg etc. are being investigated. Li, Na, and K are highly active metals but are unstable in aqueous systems due to which non-aqueous aprotic electrolytes are widely employed [27]. However, Al, Mg, Fe and Zn are relatively inactive and hence they require alkaline aqueous electrolytes during the reaction. Another component of MAB is the separator, which is used to separate two different electrolytes. It also inhibits certain mass transport processes that occur between the electrodes and prevent the short-circuit caused mainly by the metal dendrites [17,18]. A characteristic open cell structure in MAB draws oxygen from the cathode active material which is continuously supplied from an external source i.e., air [28,29]. The metal anode comprises of alkali metals (commonly Li, Na and K) or alkaline earth metals or the first-row transition metals like Fe and Zn, which possess high electrochemical equivalence. The working principle of a MAB is based on the transformation of metals or alloys into metallic ions at the anode, while, the conversion of oxygen to hydroxide ions at the cathode [30].

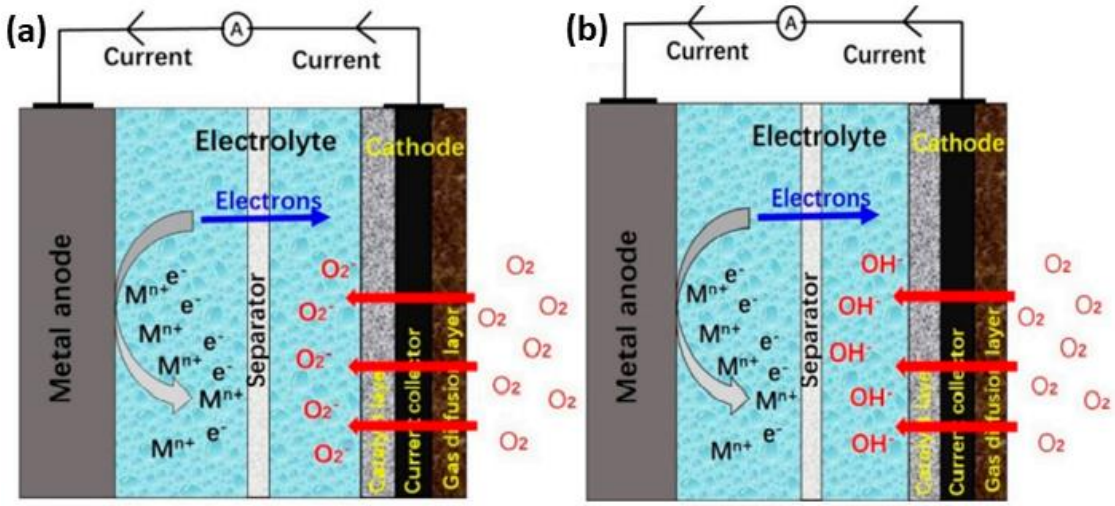

Figure 1.5. Schematic diagrams of MABs working principles for (a) non-aqueous electrolyte, and (b) aqueous electrolyte (Adapted with permission from [30]).

The choice of the electrolyte, whether aqueous or non-aqueous; depends on the nature of the anode used. A redox reaction between the metal and oxygen from the air is responsible for the generation of electricity in MABs [18]. Figure 1.5 (a,b) schematically represents the working principle of an aqueous and a non-aqueous MAB. When an aqueous electrolyte is used, oxygen diffuses through the GDL towards the battery, thereafter forming oxygen anions after combining with the electrons. In the case of non-aqueous electrolytes, oxygen molecules simply converted to its corresponding ions after receiving the electrons [30].

The chemistry involved in MABs is the conversion between molecular O_2 and its reduced forms reversibly via a one, two, or four-electron processes. The preferred pathway depends on the relative stability of the intermediates and the products formed [31]. In MABs, both metal and oxygen participate in the electrochemical reactions. The fundamental reactions involved are as follows [30]:

$$\text{At anode: } M \leftrightarrow M^{n+} + ne^- \qquad (1.4)$$

$$\text{At cathode: } O_2 + 2H_2O + 4e^- \leftrightarrow 4OH^- \qquad (1.5)$$

The electrode reactions are well-dependent on the metal electrodes, ECs as well electrolytes used [17]. An ideal electrolyte should fulfill certain properties like non-toxicity, low moisture absorption, low volatility, high boiling point, high oxygen

solubility etc. The ORR proceed via two different mechanisms, namely, a $4e^-$ pathway and a $2e^-$ pathway based on the oxygen adsorption species. When two O atoms bind to the catalyst surface, the O_2 adsorption is supposed to follow the 4e pathway. The half-cell reactions can be represented as follows [32]:

$$O_2 + 2H_2O + 2e^- \rightarrow 2OH_{ads} + 2OH^- \quad (1.6)$$

$$2OH_{ads} + 2e^- \rightarrow 2OH^- \quad (1.7)$$

$$\text{Overall: } O_2 + 2H_2O + 4e^- \leftrightarrow 4OH^- \quad (1.8)$$

When only one O atom is adsorbed on the surface of the catalyst, the favoured pathway is the $2e^-$ pathway.

$$O_2 + H_2O + e^- \rightarrow OH^- + OH_{2,ads} \quad (1.9)$$

$$OH_{2,ads} + e^- \rightarrow OH_2^- \quad (1.10)$$

$$\text{Overall: } O_2 + 2H_2O + 2e^- \rightarrow OH^- + OH_2^- \quad (1.11)$$

ORR in the air electrode, being a slower reaction, is the rate-determining step. Hence, effective ECs are required to accelerate its rate and lower its overpotential. Higher is the overpotential, lower will be output performance and energy storage efficacy. Other important factors that affect the reaction rate are the high mass transport, low rate capability, poor round-trip efficiency, low Coulombic efficiency and inadequate cycle-life [33]. All these difficulties can be resolved by rational designing of materials with high catalytic activity.

1.2.3. Challenges in PEMFCs and MABs

Despite the tremendous research for the advancement of PEMFCs and MAB technology over the last decades, several technical hurdles must be resolved before the commercial execution of the concept. For example, the cost of the individual components in PEMFC severely restricts the way of commercialization of the device. It is reported that ECs and GDL alone hold upto 61 % of the total cost of PEMFC. Whereas, the remaining 39% is covered by the PEM, bipolar plate etc. [34]. Similarly, the high cost of ECs impedes the prospects of commercialization of MABs. Additionally, both FCs and MABs associated with several technical challenges. The activity of rechargeable MABs is fundamentally assessed from the recharging and discharging efficiency of the device [17]. The up-gradation of the MAB operation dealing with both efficient discharge and rechargeability remains a great challenge.

The key issues that counter MABs commercialization are associated with the inadequate functionality of metal anodes, air cathodes, and electrolytes. Consequently, it is vital for endorsing further advancement in the MABs to resolve the key challenges from the approach of materials science, exploring the material design of metal electrodes, air electrodes, electrolyte, and separator materials. Figure 1.6 presents the schematic scenario for current issues and material design strategies for the advancement of MAB performances.

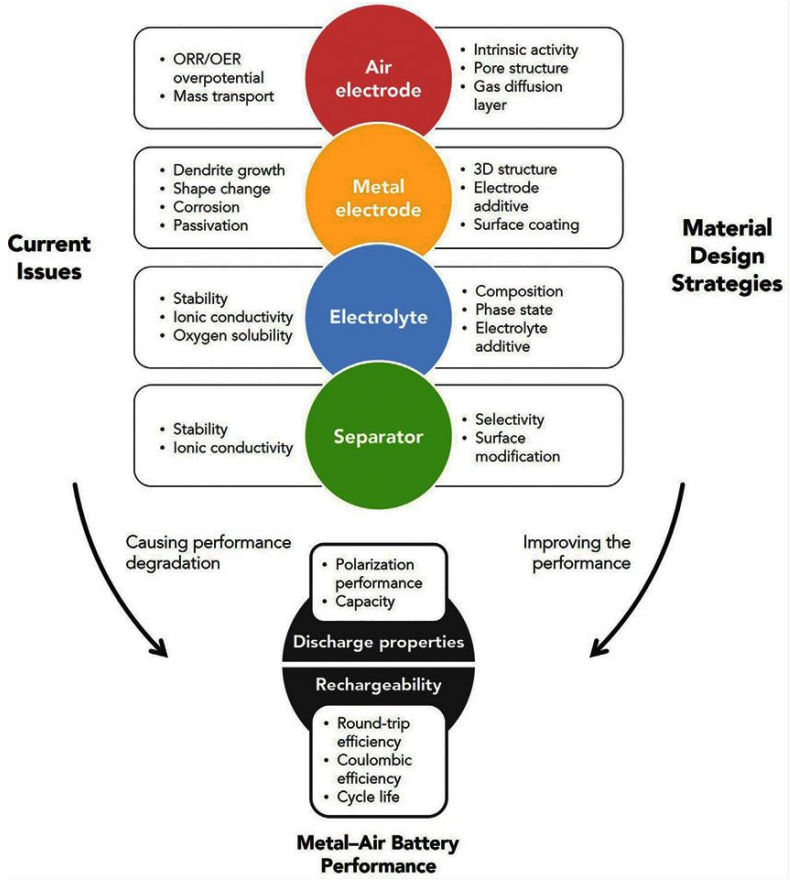

Figure 1.6. Evaluation parameters, material challenges, and material design strategies for MABs (Adapted with permission from [17]).

1.3. Oxygen Reduction Reaction (ORR)

ORR is one of the most crucial redox processes in electrochemical energy converting systems such as FCs, MABs etc. The ORR process comprises several steps with the exchange of H^+ and e^- on the cathode surface. The overall reaction is merely the electrochemical interconversion between H_2O, H_2O_2 and O_2. However, it is

multifaceted and involves many steps with different intermediates (e.g., O*, OH*, OOH* etc.) which are difficult to determine experimentally depending on the electrolyte, nature of the ECs and oxygen coverage [35–38]. Figure 1.7 shows the likely interconversion of these intermediates throughout the ORR process which makes the mechanism appallingly complex. For instance, ORR typically proceeds through two different pathways in both acidic and alkaline media. Table 1.1 shows the characteristic ORR pathways along with thermodynamic reaction potential exhibited in the respective electrolyte [37]. A "direct" reduction of molecular O_2 is a $4e^-$ process. However, the electrolyte has a significant impact on the reaction potential as is

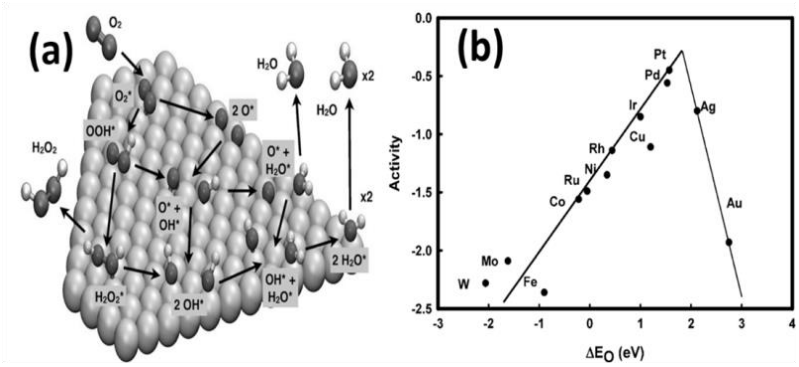

Figure 1.7. (a) Schematic representation of various possible ORR intermediate and mechanisms (Reproduced with permission from Ref. [36]) and (b) ORR volcano plot for metals. (Adapted with permission from Ref. [35]).

apparent from Table 1.1. The "indirect" O_2 reduction is a two-step process that produces H_2O_2 as an intermediate product and is considered a cost-effective strategy for H_2O_2 generation. Intermittently, the HO_2^- and H_2O_2 formed via the $2e^-$ pathway can undergo an alternate decomposition process and can lead to the formation of OH^-, O_2 (in alkaline media), H_2O and O_2 (in acidic media) as shown in Table 1.1. Nevertheless, the "direct" $4e^-$ pathway is comprehended for efficient ORR since H_2O_2 produced in the $2e^-$ pathway diminishes the energy-conversion efficiency and triggers the disintegration of the H^+-conducting polymer electrolyte in PEMFCs.

The nature of the ECs has a greater impact on the ORR routes as it not only depends on the O_2 adsorption but also the O^{2-} surface interactions over the ECs. For example, the theoretically constructed ORR volcano plot (Figure 1.7 b) studied on

different metal surfaces demonstrates the electrocatalytic activities shown by metal ECs as a function of ΔE_o (eV), suggesting the correlation of free energies of oxygen intermediate binding to the metal surfaces. In addition, numerous investigations have exposed the 'oxygen coverage' as a critical descriptor for ORR mechanisms. Nørskov *et al.* comprehensively reported the 'oxygen coverage' dependence of ORR mechanisms by employing the density functional theory (DFT) approach [35,38].

Table 1.1: ORR pathways on working electrode [37].

Electrolyte	Reaction	Reduction Potential (V vs. NHE)
Aqueous–Alkaline	$4e^-$ Pathway:	
	$O_2 + 2H_2O + 4e^- \rightarrow 4OH^-$	+0.401
	$2e^-$ Pathway:	
	$O_2 + H_2O + 2e^- \rightarrow HO_2^- + OH^-$	–0.065
	$HO_2^- + H_2O + 2e^- \rightarrow 3OH^-$	+0.867
	or decomposition:	
	$HO_2^- \rightarrow 2OH^- + O_2$	
Aqueous–Acidic	$4e^-$ Pathway:	
	$O_2 + 4H^+ + 4e^- \rightarrow 2H_2O$	+1.229
	$2e^-$ Pathway:	
	$O_2 + 2H^+ + 2e^- \rightarrow H_2O_2$	+0.67
	$H_2O_2 + 2H^+ + 2e^- \rightarrow 2H_2O$	+1.77
	or decomposition:	
	$2H_2O_2 \rightarrow 2H_2O + O_2$	

The study showed that at high O_2 coverage, the formation of OOH* occurs first followed by O–O bond cleavage (an associative mechanism); whereas at low O_2 coverage, OH* is formed after the O–O bond cleavage (a dissociative mechanism). The associative mechanism in both acidic and alkaline media can be expressed through

the following elementary steps (* stands for the ECs surface free site, (l) and (g) denote liquid and gas phases, respectively, and O*, OH* and HOO* are the EC adsorbed intermediates):

In acidic media:

$$O_2\,(g) + * \rightarrow O_2* \quad (1.12)$$

$$O_2* + H^+ + e^- \rightarrow HOO* \quad (1.13)$$

$$HOO* + H^+ + e^- \rightarrow O* + H_2O\,(l) \quad (1.14)$$

$$O* + H^+ + e^- \rightarrow HO* \quad (1.15)$$

$$HO* + H^+ + e^- \rightarrow H_2O\,(l) + * \quad (1.16)$$

In alkaline media:

$$O_2\,(g) + * \rightarrow O_2* \quad (1.17)$$

$$O_2* + H_2O\,(l) + e^- \rightarrow HOO* + OH^- \quad (1.18)$$

$$HOO* + e^- \rightarrow O* + OH^- \quad (1.19)$$

$$O* + H_2O\,(l) + e^- \rightarrow HO* + OH^- \quad (1.20)$$

$$HO* + e^- \rightarrow OH^- + * \quad (1.21)$$

The dissociative mechanism can be expressed through the following elementary steps:

$$O_2\,(g) + * + * \rightarrow O* + O* \quad (1.22)$$

followed by steps (1.15) and (1.16) in acidic media or (1.20) and (1.21) in alkaline media.

A characteristic ORR polarization curve measured by linear sweep voltammetry (LSV) is shown in Figure 1.8. It has three distinct regions which are classified as kinetically controlled, mixed kinetic-diffusion controlled and diffusion-controlled regions [39]. The ORR rate at the kinetically controlled region is essentially lower; hence producing small currents. The combined kinetic and diffusion control region is associated with faster and increased current with a substantial rise in overpotential. The current obtained in the diffusion-controlled region is constant which is dependent on the rate of diffusion of the reactant molecule. The ORR onset potential (E_{onset}) is an important electrochemical parameter which describes the maximum

potential values at which a reaction product is formed at the cathode in defined conditions. A more positive ORR E_{onset} indicates the requirement of lower overpotential to obtain the reaction product. Half-wave potential ($E_{1/2}$) is another characteristic parameter used for the ORR activity assessment, which is the potential at which polarographic wave current is equal to one-half of diffusion current.

The kinetic current density (j_K) is calculated using Koutecky–Levich (K–L) equation [45], as shown in equation (1.23), where, j is the measured current density, j_k is the kinetic current density which is independent of mass transfer, j_d is the diffusion current density, ω is the angular rotation speed of the WE, n is the number of electrons transferred during ORR, F is the Faraday constant (96485 C mol^{-1}), C_0 is the bulk concentration of dissolved O_2 (1.2×10^{-6} M cm^{-3}), D_0 is the diffusion coefficient of O_2 (1.9×10^{-5} cm^2 s^{-1}), v is the kinematic viscosity of the electrolyte (0.01 cm^2 s^{-1}). As per the equation, the intercept and slope of the plot of j^{-1} *vs.* $\omega^{-1/2}$ give the values of j_K and n, respectively.

$$\frac{1}{j} = \frac{1}{j_k} + \frac{1}{j_d} = \frac{1}{j_k} + \frac{1}{B\omega^{1/2}} \qquad (1.23)$$

$$B = 0.62nFC_0(D_{02})^{2/3}v^{-1/6}$$

$$j_k = nFkC_0$$

1.4. Oxygen Evolution Reaction (OER)

OER is a process of producing molecular oxygen (O_2) through a chemical mechanism such as observed in the oxidation of H_2O during oxygenic photosynthesis, splitting of H_2O into O_2 and H_2 etc. The electrochemical H_2O splitting has been a familiar phenomenon for a long. In the 19th century, William Nicholson and Anthony Carlisle demonstrated one of the most inspiring scientific discoveries ever made out, revealing that electrical energy can split H_2O into H_2 and O_2 [40]. However, the OER that takes place at the anode of H_2O electrolyzers, is still an enigma [41]. The precise OER reaction mechanism and the ideal ECs for the reaction in terms of activity, stability and durability still remains unclear. OER is a vital process in energy conversion and storage devices, particularly in water electrolysis, regenerative FCs and MABs. Technically, electrochemical OER is an O–O bond formation process at the

anode which involves a $4e^-/H^+$ couple and hence the reverse of ORR [41]. Resembling ORR an elementary OER process also needs a total transfer of $4e^-$ that accomplishes through the multi-step mechanism. As a consequence, the kinetics of OER is sluggish and that affects the overall efficiency of an energy-converting device [42]. Depending on the pH of the electrolyte the OER redox process can be different. In an alkaline solution, OH^- ions are oxidized to O_2 and H_2O, while in an acidic solution O_2 and $4H^+$ are produced from two molecules of H_2O [43]. The corresponding anodic half-reactions at STP are as follows:

In alkaline medium: $4OH^- \leftrightarrow 2H_2O\,(l) + O_2\,(g) + 4e^-$; $E_a° = 0.404$ V vs. RHE (1.24)

In acidic medium : $2H_2O\,(l) \leftrightarrow O_2\,(g) + 4H^+ + 4e^-$; $E_a° = 1.23$ V vs. RHE (1.25)

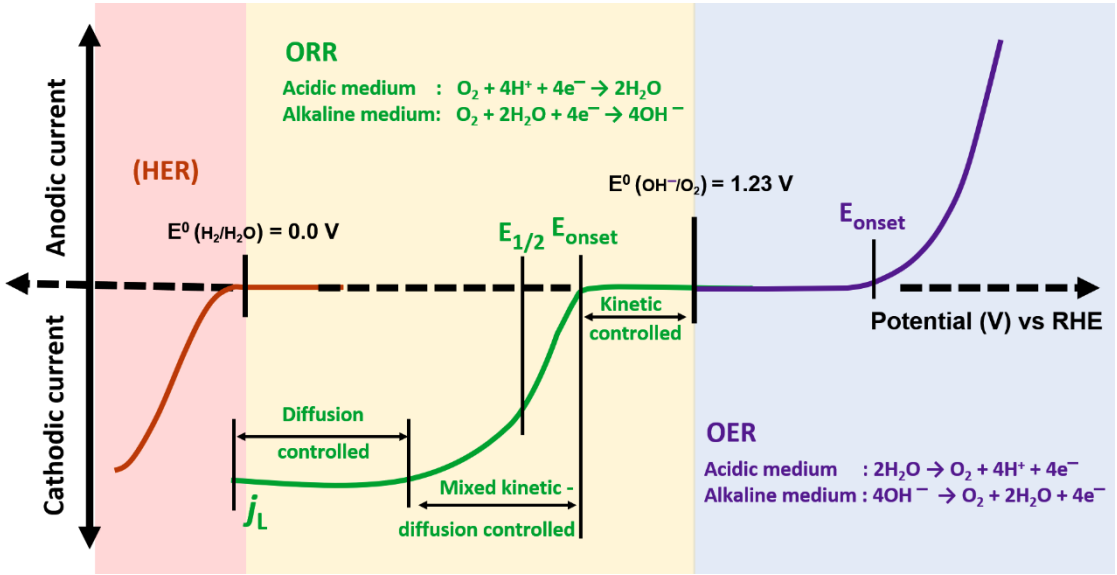

Figure 1.8. The characteristics of ORR and OER polarization curve and the key parameters.

A typical OER polarization curve measured by the LSV technique is shown in Figure 1.8. The kinetics of OER are usually assessed through Tafel slope, potential (Ej_{10}) and the overpotential at a current density of 10 mA cm^{-2} (η_{10}) [42]. A lower Tafel slope and lower overpotential values are characteristics of a better OER EC [43]. Electrochemically active surface area (ECSA) is a significant parameter of an EC, which offers the electrochemically available active sites for ORR/OER. ECSA can be evaluated from the double-layer capacitance (C_{dl}), calculated in the non-faradaic region of the CV plot.

1.5. Recent Advancement and Challenges of ECs for ORR

The cathodic reaction in PEMFCs and MABs is essentially the ORR. Notably, the overall efficiency of the device is controlled by ORR. It is typically regarded as the rate-determining zone due to its sluggish kinetics, caused by the O_2 adsorption difficulties on the electrode surface, O–O bond cleavage/activation and removal of oxide [35,44]. Electrocatalysis is the most anticipated methodology for the escalation of ORR kinetics [45]. At the current stage in FC technologies, Pt-based nanostructured materials are being used as the cathode EC. However, Pt-based catalysts have some critical issues such as cost, stability, durability, etc. Consequently, there is a substantial need to explore alternative cathode catalysts to overcome these issues [46–48]. In recent times, nanostructures (NSs) including transition metal oxides (TMOs), mixed metal oxides (MMOs), metallic alloys, perovskites, metal-organic frameworks (MOFs), etc. supported on various carbonaceous materials have been extensively investigated as cathode catalysts [49–52]. Owing to their synergistic effect, high O_2-diffusion capability, anionic defects and significant hetero-structure interfacial mechanism of supported nanoparticles (NPs) exhibit superior electrocatalytic activities. Consequently, systematically modified NPs have attracted growing interest in the advancement of ORR ECs [49–57].

Following the all-possible pathways, the scientific community is in search of the precise rate-determining step. Nie *et al.* suggested that the ORR kinetics on metal surfaces are primarily controlled by three steps: (a) the first electron exchange of the ORR, (b) the hydration of O_2, and (c) the desorption of the intermediates [58]. Based on the reports from the present scenario, it is evident that the enhancement of kinetics and the downswing of overpotential for ORR in both alkaline and acidic media demand a 'direct' $4e^-$ pathway without the outgrowth of H_2O_2 for efficient outcome. As mentioned above, electrocatalysis is the most viable tactic to lead an efficient ORR process. Numerous materials have been employed and tested as cathode ECs to date [35]. The theoretical approach demonstrates Pt as the best ORR ECs which is apparent from the ORR volcano plot (Figure 1.7b). However, as observed from the volcano plot, it leaves significant scope for the future ECs which can meet the "apex of the volcano".

1.6. Recent Advancement and Challenges of ECs for OER

The theoretical redox potential value of the OER is 1.23 V (vs. RHE) at STP in all electrolyte medium [59]. As OER is a very sluggish process, it needs a higher potential than the theoretical potential (i.e., high overpotential) to overcome the total energy barrier [60]. The efficiency of FCs, MABs and water splitting devices is critically dependent on the OER and ORR activities [61]. Consequently, the design of effective and stable ORR/OER EC with higher activity is crucial for overcoming the kinetic barriers and enhancing the overall energy-conversion efficiency. Elementary research on EC for OER started in the 19th century when noble metals (e.g., Pt, Pd, Ru, Ir and Rh) and subsequently noble-MOs (e.g., IrO_2, RuO_2) were employed as active ECs in both acidic and alkaline conditions [62,63]. However, because of the low abundance and high cost of these metals the commercial execution of the ECs are still restricted. Consequently, considerable research efforts have been undergoing for the last two decades in the search for low-priced, high activity and sustainable ECs as alternatives [64]. TMOs and other oxides including spinels, perovskites and layered hydroxides (MOOH, $M(OH)_2$ $LiMO_2$ where M = Mn, Fe, Co and Ni) etc. are observed to be highly active for OER [42]. Yoo *et al.*[65]. revealed the effect of participation of lattice oxygen in perovskites to carry out OER. Approaching with density functional theory (DFT) calculation, they showed that OER via lattice [O] mechanism revealed better activity than traditionally used adsorbate evolving mechanism. Recently, Chen *et al*. [66]. reported Ce modified-CuO_x synthesized by electrodeposition technique with enhanced OER activity. In 2020, Wu and co-workers [67] reported a facile fabrication outline for Co_3O_4@CoO@Co (gradient core@shell) NPs on graphene to study their electrocatalytic potentials for an OER and ORR in alkaline electrolytes. To study the effect of substitution in the crystal lattice, Karmakar *et al.* [68] designed a one-step hydrothermal fabrication of graphite paper (GP)- supported cobalt carbonate hydroxide ($Co_2(CO_3)(OH)_2$/GP) nanostructures and its Ni- and Mn-substituted products, $Co_{1.9}Ni_{0.1}(CO_3)(OH)_2$/GP and $Co_{0.95}Mn_{0.05}CO_3$/GP, respectively. It is noteworthy that Ni- and Mn-substituted $Co_2(CO_3)(OH)_2$ exhibited significantly enhanced OER performance in 1.0 M KOH. Similarly, Wang and co-workers [69] studied Fe- doped Cobalt carbonate hydroxide hydrate nanowires grown on nickel foam (denoted as Fe-CCHH/NF) to obtain effective OER catalysis by electrochemical

transformation. The Fe-CCHH/NF-30 displays OER catalytic activity with an overpotential of only 200 mV (vs. RHE) at a current density of 10 mA cm^{-2} and a small Tafel slope of 50 mV dec^{-1} in 1M KOH.

1.7. Development of Bifunctional ECs for ORR/OER

The design of bifunctional ORR/OER ECs can promote both discharge and charge processes of URFCs and MABs. A competent bifunctional EC is needed to enhance the ORR/OER rate and to reduce the overpotential as the normal kinetics of the oxygen reaction are inadequately vigorous. In MABs, the ORR and OER are taking place at the air electrode (cathode), where ORR takes place throughout the discharge cycle while OER occurs during the charge cycle. Numerous ECs systems, including noble metal-based materials (such as Pt, Pd, IrO_2, RuO_2 etc.), metallic alloy, TMOs, MMOs, perovskites, metal organic frameworks (MOFs), etc. anchored on different carbonaceous materials have been extensively studied as cathode catalysts [19].

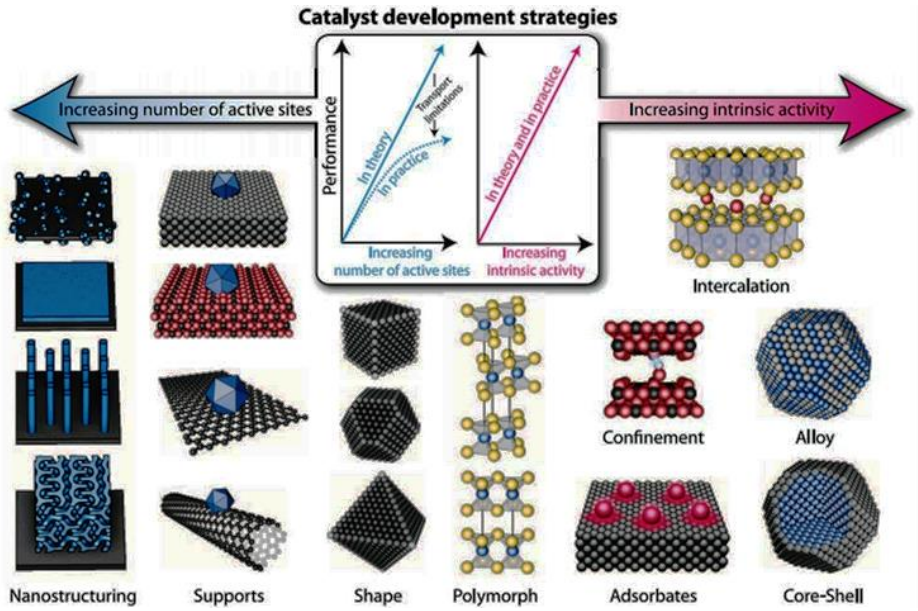

Figure 1.9. Development strategies for metal catalysts. (Adapted with permission from reference [70].

Figure 1.9 shows the different development strategies for metal-based catalysts to further enhance the active sites and the intrinsic activities. To date, Pt-group metal-

based materials such as Pt and Ir-/Ru-based alloys or oxides have been established to be highly active in oxygen electrocatalysis [71–73]. Nevertheless, noble metal catalysts are mostly incompetent to bifunctional activity, thus obstructing their application in regenerative energy-converting devices. Consequently, the development of high-performance non-precious metal-based bifunctional ECs is crucial for practical application. In recent times, non-noble MO based composites have attracted massive attention as the bifunctional oxygen ECs owing to inexpensive, abundant, and high activity toward ORR and OER. Because of the high O_2-diffusion capability, synergistic effect, anionic defects and significant hetero-structure interfacial mechanism, these materials demonstrate excellent electrocatalytic activities. To facilitate the maximized electrocatalytic efficiency, the research community is further concentrating their work on the suitable morphological and structural engineering of the catalyst materials which will be summarized in this section.

1.7.1. Metal Oxide-Based ECs

MO ECs include the oxides of noble metals, TMO, MTMOs, inner transition metals, perovskites, spinel etc. MOs with different stoichiometric or even non-stoichiometric compositions have recently attracted growing research interest worldwide. Benefiting from their adjustable chemical constitution, structural diversity, easy preparation, and astonishing synergistic and electrochemical properties, these materials play significant roles in environmentally friendly energy storage/conversion technologies [72]. Additionally, offering greater scope for cultivation of the intrinsic activity with structural engineering for high electrochemically exposed surface area, MOs can be a potential candidate as the ECs for H_2O electrolyzers, URFCs and MABs.

1.7.2. Noble Metal Oxides

Noble metals such as Au, Pt, Ag, etc. usually have little tendency to unite with O_2 in the free state and under red heat conditions, they may react with and do not alter their composition. Noble metal oxides are readily decomposed by heat as a consequence of the weak affinity between the metal and oxygen. It is noteworthy that, Pt-based materials are highly active toward ORR, while RuO_2 and IrO_2 are well recognized to be active toward OER and regarded as the state-of-the-art OER EC [71–

73]. Nevertheless, RuO_2 and IrO_2 are less active towards ORR, on the contrary, Pt-based materials are less active towards OER, and hence they are not efficient as bifunctional ECs for ORR and OER.

1.7.3. Non-Noble Metal Oxides

1.7.3.1. Single Metal Oxides

Single MOs i.e., oxides with identical metal centres can be classified into this category. These materials show significant activity and stability in the alkaline medium for ORR and OER [74]. For example, TMOs of the type M_xO_y (M= Mn, Fe, Co, Ni etc.) supported on carbon are observed to be highly active toward oxygen electrocatalysis. Manganese oxides (Mn_xO_y) have attracted the researcher because of their flexible valences and plentiful structures, giving rise to rich redox couples. As an illustration, Cheng *et al.* reported the electrocatalytic activities of MnO_2 correlating with the crystallographic structure, following the order of α-> β-> γ-MnO_2 [75]. Gorlin *et al.* designed a thin-film analogue consisting of a nanostructured Mn(III) oxide by using an electrodeposition technique that exhibits an excellent electrocatalytic activity for the ORR and OER in alkaline solution [76]. Its bifunctional ORR/OER performance is comparable to that of noble metal catalysts. Furthermore, apart from Mn_xO_y, other single MOs such as Fe_xO_y, NiO, CuO and Co_xOy were also demonstrated to be efficiently active toward the electrochemical oxygen reaction [74,77,78].

1.7.3.2. Spinel

Spinel-type oxide is one of the most significant bifunctional O_2 ECs among TMOs. Typical spinel oxides can generally be designated as group oxides with the formula AB_2O_4, where A and B stands for divalent and trivalent metal ions, respectively and their structure is assembled upon a cubic close-packed array of O^{2-} ions, where A(II) cations usually occupy the parts or all tetrahedral sites and B(III) cations occupy octahedral sites. Based on the spatial distribution of A(II) and B(III) cations in the unit cells, spinel oxides can be classified as normal, inverse, and complex spinel oxides. Owing to its exceptional crystal structure it can provide effective catalytic active sites for both ORR and OER. Hence, the structure of spinel oxides has a straight connection to the ORR and OER performance. Many researchers

have been working on the fine-tuning and structural design of spinel oxides directing from different aspects. Rational doping in A/B sites, designing oxygen vacancy defects, adjusting the crystal plane and structure, morphology-controlled synthesis etc. are some fascinating methodologies that can be used to modulate the spinel oxides to enhance the ORR/OER performance. Recently, Han *et al.* synthesized morphology-controlled Co_3O_4 (cubic, octahedron, and polyhedron) nanocrystals anchored on N-doped reduced graphene by a simple template-free hydrothermal method [79]. Nanostructured Co_3O_4 polyhedrons with the major exposed facets of (112) displayed greater ORR/OER performance relative to that of cubic and octahedron Co_3O_4 nanocrystals due to the different surface abundance of Co^{3+} and Co^{2+} active sites. It was suggested that the greater population of octahedrally coordinated Co^{3+} on (112) planes boosted the adsorption, desorption and dissociation properties of O_2 species, which enhances the activity. Similarly, Li *et al.* synthesized a three-dimensional flower-like heterostructure of $NiCo_2O_4$ with N-doped carbon derived from g-C_3N_4, under a hydrothermal approach [80]. The $NiCo_2O_4$-CN displays improved ORR activity with a half-wave potential ($E_{1/2}$) of 0.81 V and high OER activity with a smaller overpotential (383 mV). In a test with a Zn-air battery, the $NiCo_2O_4$-CN shows similar performance to the commercial Pt/C and IrO_2. The enhanced bifunctional ORR/OER activity is attributed to the combined effects of porous 3D structure, high electrochemically active surface area (ECSA) and abundant oxygen vacancies incorporated in the catalyst. Mixed valence spinel oxides have also been observed to bifunctionally active toward oxygen electrocatalysis. In the late 90s, Rios *et al.* reported the ORR/OER activity of the $Mn_xCo_{3-x}O_4$ [81]. Similarly, mixed-valence spinel oxides such as $Cu_xCo_{3-x}O_4$, $Ni_xCo_{3-x}O_4$, $CoMn_2O_4$ etc. have also been well demonstrated as efficient bifunctional ORR/OER activity.

1.7.3.3. Perovskites

Perovskites are a class of unique MOs that are bifunctionally active for ORR and OER. They can be typically represented as ABO_3, where A usually represents a positively charged rare earth metal or alkaline earth metal cation and B is a TM ion with a charge that is more positive relative to A. The perovskite unit cell comprises BO_6 octahedrons where A introduced in the void among the BO_6 structures. Perovskite

has extensive flexibility for engineering the crystal structure relative to spinel oxides as almost all kinds of metallic elements (more than 90% metallic element) can be doped into perovskite structures and a large range of oxygen non-stoichiometry is allowed and because of these characteristic features perovskite have been largely studied for the advancement of their bifunctional ORR/OER performances. Modification of the cation in A/B sites has been an effective technique to tune the electronic structure, which generates verities of redox couple and lattice defects in perovskite oxides. For instance, Lee *et al.* designed Ni-doped Co-based double perovskites ($PrBa_{0.5}Sr_{0.5}Co_{1.9}Ni_{0.1}O_{5+\delta}$, PBSCN1) employing sol-gel and combustion technique [82]. The doping of Ni triggered the coexistence of Co cations with various oxidation states with enlarged surface sites for O_2 adsorption/desorption thereby exhibiting enhanced OER activity. Analogously, Fe-doped $PrBa_{0.5}Sr_{0.5}Co_{1.5}Fe_{0.5}O_{5+\delta}$ nanofibers were formulated via electrospinning [83]. The mesoporous $PrBa_{0.5}Sr_{0.5}Co_{1.5}Fe_{0.5}O_{5+\delta}$ nanofiber displayed high ORR and OER activity with enhanced stability in the Zn-air battery.

1.7.3.4. Other mixed metal oxides

Heterostructures containing one oxide on another oxide are kind of unique MOs that have several implications in catalytic industries including oxygen electrocatalysis. Taking into account catalytic chemists, MMOs are oxygen-containing unifications of two or more metallic ions in proportions that may either vary or be defined by strict stoichiometry. They are usually attained in the form of powder or single crystals. MMOs are characteristics of rich oxygen defects, multivalent redox and oxide-oxide interfacial phenomenon. Owing to these properties non-noble MMOs exhibit excellent bifunctional ORR/OER performance and stand as a promising alternative to expensive Pt-based ECs. Recently, Liu et al synthesized Co_3O_4-CeO_2/KB using a simple two-step hydrothermal method as a high-performance ORR catalyst for Al-air batteries [84]. The activity and stability of Co_3O_4/KB toward ORR were notably amplified when it was mixed with CeO_2 NPs. Goswami et al reported the synthesis of CuO_x-CeO_2/C rich oxide−oxide and oxide−carbon interfaces that exhibited high bifunctional ORR/OER activities in an alkaline medium [49]. Figure 1.10 show the TEM and HRTEM images of the lattice spacing incorporated with characteristics of

oxide-oxide and oxide-carbon interface structure, the particle size distribution of CuO_x-CeO_2/C along with the ORR/OER performance exhibited by the EC. The higher ORR/OER performance of CuO_x-CeO_2/C was attributed to the synergistic effects, enriched oxygen vacancies owing to the presence of $Ce^{4+}/Ce^{3+,}$ abundant oxide−oxide and oxide−carbon heterointerfaces, and regular distribution of oxides over the carbon matrix that facilitates faster electronic conduction. Wang and coworkers synthesized another type of MMO, $CoNiO_2$/SNC nanocomposites with the unique waxberry-like hollow architecture as trifunctional ECs for OER, ORR, and HER [85]. The EC demonstrates remarkable activity for OER, ORR, and HER in an alkaline medium.

1.8. Tailoring the Structure of Metal Oxide-Based ECs.

1.8.1. Morphology

It is well-recognized from the crystallographic correlations, that the shape of NP strongly influences the pattern of the atoms at its surface; i.e., its structure. The catalytic behaviour of a material is inherently related to the structural shape and size of the catalyst. Hence, the shape and size control of MOs are considered an influential command for manoeuvring the properties of MOs towards oxygen electrocatalysis [86]. However, the correlation between morphology and electrocatalysis has not been well explored or understood yet. Zhang et al, investigated Cu_2O with three different morphologies (sphere, octahedron and truncated octahedron) using the potentiostatic electrodeposition technique [87]. The ORR performance exhibited by the Cu_2O with truncated octahedron shape was found to be superior and based on the comprehensive study of electrocatalysis experiments and DFT calculations, it was observed that truncated Cu_2O octahedron preferentially exposes the (100) facet, which is favourable to effective adsorption and activation of O_2 on the surface of Cu_2O. Similarly, Yang and the group reported single-crystal $(Mn,Co)_3O_4$ octahedra, synthesized via a precipitation-ageing process [88]. Based on the Mn/Co ratio the $(Mn,Co)_3O_4$ octahedra expose (111) and (011) facets of cubic and tetragonal phases, respectively. The single-crystal octahedra of Mn_2CoO_4 and $Mn_{2.5}Co_{0.5}O_4$ with (011) facets exhibited efficient selectivity towards ORR in an alkaline medium.

1.8.2. Doping

The methodical doping of species into host structures technique has long been applied to modify the electronic, magnetic, and physical structure of semiconductors to increase their working efficiency [89]. Likewise, in catalytic systems, the selective metal doping into a MO matrix can result in the establishment of a large number of structural defects such as oxygen vacancies and interstitial defects etc.[90] which is of great importance in industrial catalytic processes including oxygen electrocatalysis. Owing to this, tuning the MOs with the doping method has become a potential technique for the development of advanced oxygen ECs. For instance, Zhang *et al.* reported Ru-doped NiO/Co_3O_4 heterostructure as an advanced trifunctional ECs for ORR/OER/HER [91]. The catalyst produced a current density of 100 mA cm^{-2} in alkaline solution at only 269 mV vs. RHE (OER) overpotential and a high half-wave potential of 0.88 V (ORR). In a test for the water-splitting device, the catalyst can function steadily for a longer duration (> 40 h), which is better than Pt/C and RuO_2 at high current densities.

1.8.3. Oxygen Vacancy and Defects

Defect engineering is an inspiring strategy for fabricating highly efficient and stable ECs that have recently attracted widespread research attention. It can either modulate the adjacent electronic structure of defect sites for controlling activation energy of various adsorbed intermediates or serve as ‘‘docking’’ sites to stabilize the atomic moieties and form an additional unique synergetic coordination assembly as the active sites [92]. Defects in nanomaterials are usually recognized as the active sites for electrocatalytic processes because of the exceptional electronic and surface properties in the local vicinity. Defects in MOs are synonymous with cationic or anionic defects, broadly which is characterized as oxygen vacancy and metal vacancy. In ORR/OER electrocatalysis, oxygen vacancy plays a crucial role in providing plentiful adsorption sites for a competent catalysis process. Consequently, defect engineering has been broadly implemented for fabricating MOs to enhance their electrocatalytic reactions.

1.8.4. Interface Engineering

In heterogeneous catalyst systems, interfaces are the edges between adjacent substances of the catalyst material which possess unavoidable defects that make it

unique characteristics relative to its parent materials. Recently, interface engineering of MO-based heterostructures has received massive attention as it has been recognized as an important strategy for the design and advancement of oxygen ECs. The interface in heterostructures provides a broader scope for modulating the reaction environment such as optimization of chemisorption for reaction intermediates, controlling the electron/mass transportation, and preventing active components from aggregating [93]. Interface engineering is accomplished by the building of heterojunction. The process involves the integration of different components such as metal-metal, metal-oxide, oxide-oxide, oxide-hydroxide and metal-non-oxide (e.g., carbon, phosphate, chalcogenide, nitride and carbide). A typical interfacial catalyst system of CuO_x and CeO_2 anchored on a carbon bed (CuO_x-CeO_2/C), was synthesized by Goswami *et al.* using a facile hydrothermal approach as shown in Figure 1.10. The HRTEM image reveals the interfaces which are not only between C (002) and CeO_2 (111) facets but also the oxide-oxide interface within CeO_2 (200) and CeO_2 (111) facets exposing abundant active sites for a favourable electrocatalytic process for ORR/OER.

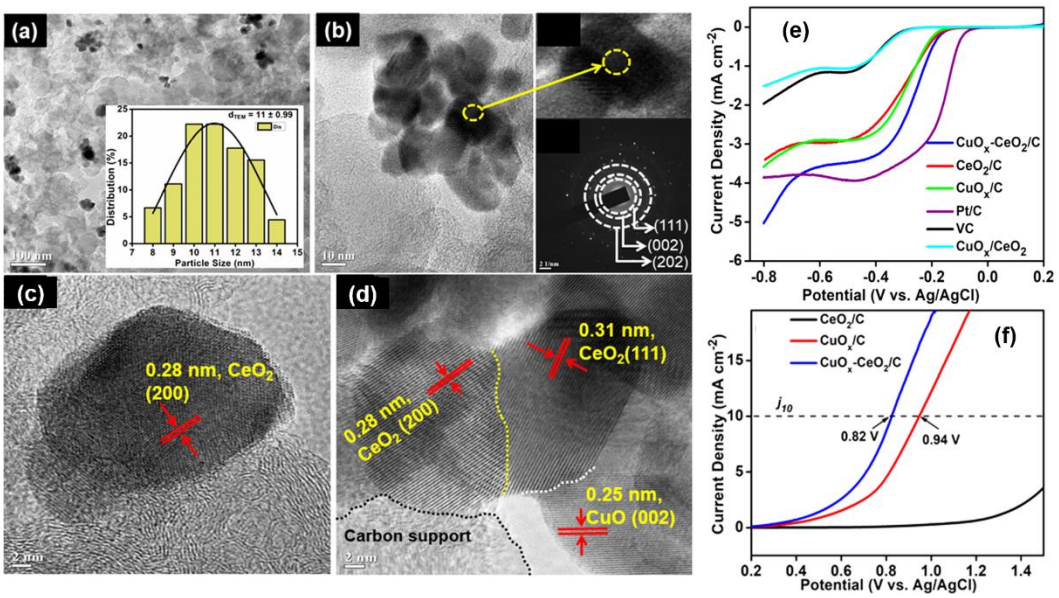

Figure 1.10. (a-d) TEM and HRTEM images with distinguished lattice fringes, particle size distribution curve (inset image (a)), SAED pattern (inset image (b)), (e) ORR LSV curves for VC, CeO_2/C, CuO_x/C, CuO_x-CeO_2/C, Pt/C, and CuO_x/CeO_2 in O_2-saturated 0.1 M KOH at 1600 rpm, (f) OER LSV curves at 1600 rpm. (Adapted with permission from [49]).

1.9. Effect of Carbon-Supported MOs for ORR/OER

Carbon-based materials such as carbon nanotube, Vulcan XC 72R, ketjenblack (KB), BP2000, graphene, etc. exhibit unique conductive as well as supportive properties that can enrich the performance of electrocatalytically active materials. These materials have been extensively investigated as a cathode component for FCs and MABs because of the low-cost, large specific surface areas, easy induction of surface groups, chemical inertness, robust nature and high electrical conductivity. [94–98]. It is observed that the carbon materials support better electrical conductivity, accelerating the charge transfer, thereby enhancing the ORR/OER activity as well as the durability of the catalyst. Furthermore, carbon supports play a significant role to modulate the physical properties of the catalysts. For example, it enhances the surface area, homogenizes the dispersion of MO particles, prevents the agglomeration of the particles, lowers the resistance of mass transportation etc.

1.10. Effect of CeO_2 Incorporation into MOs for ORR/OER

CeO_2 has unique characteristics such as high oxygen storage capability, high reactivity and hardness, high oxygen ionic conductivity, strong ultraviolet radiation absorption ability, as well as high temperature stability. Over the past few decades, CeO_2 has been utilized in different catalytic processes and has attracted enormous attention as an "active catalyst" as well as an "active supporter/promoter" [99]. Because of its fascinating Ce^{4+}/Ce^{3+} redox couple, it has been extensively used as an active catalyst/promoter in several reactions such as CO oxidation, ORR, elimination of toxic exhaust (SO_2, CO, and NOx, three-way catalyst), selective hydrogenation of unsaturated aldehydes and isobutane dehydrogenation, and as free radical scavenger [99–103]. Recently, CeO_2-promoted TMOs on carbon have been used as bifunctional ECs for ORR and OER [84,104–106].

1.11. Objectives of the Present Work

As per the present status, established from the strong foundation work executed by the researchers in the field of oxygen electrocatalysis, this is quite obvious that both the energy conversion and storage devices are still combatting the wider commercial applicability due to some major challenging issues such as higher overpotential (i.e.,

lower activity), stability and high cost of the EC used. Consequently, to resolve the cost issue of the ECs researchers are making a tremendous effort on non-precious metal oxide-based ECs. Researchers are working on the modification of the chemical and physical properties of the ECs that can reduce the overpotential, thereby enhancing the electrocatalytic activity. The synthesis of morphology-controlled non-noble metal oxide-based ECs in the supported and/or unsupported form has gained significant attention because of the potential capability to overcome some of the critical issues in this field. Achieving an excellent redox mechanism, a combination of metal oxides (i.e., MMOs) can make the EC system more efficient than the single MO alone. However, engineering such adequate structures to resolve the above-mentioned issues is rather a challenging task which leads to a broader scope to design suitable ECs in energy applications like FCs, MABs etc.

In line with that, I focused my work on the design of non-precious MO-based ECs employing simplistic methods for binfunctional ORR/OER. The primary objectives of the present work are given below:

1) To synthesize metal oxide carbon composites of type M_xO_y /C (M= Co, Fe, Mn) with emphasis on morphology control.
2) To synthesize CeO_2 promoted/supported hybrid oxides of type $M_xO_y/CeO_2/C$ (M = Mn, Fe, Cu) of different compositions.
3) To study the nanointerface, surface chemical compositions, textural, crytsalline and thermal characteristics by multi-techniques approaches.
4) To evaluate and study the structure-activity correlation of M_xO_y/C (M= Co, Fe, Mn) for ORR/OER in an alkaline media for long-term stability and durability.
5) To elucidate the role of CeO_2 in forming active, highly durable and stable ECs of type $MO_x/CeO_2/C$ (M = Mn, Fe, Cu) for ORR/OER in alkaline media.

References

[1] Jha, S. K., Bilalovic, J., Jha, A., Patel, N., and Zhang, H. Renewable energy: Present research and future scope of artificial intelligence. *Renewable and Sustainable Energy Reviews*, 77:297-317, 2017.

[2] Torres, D. J., and Crichigno, J. Influence of reflectivity and cloud cover on the optimal tilt angle of solar panels. *Resources*, 4(4):736-750, 2015.

[3] Segura, F., and Andújar, J. M. Modular PEM fuel cell SCADA & simulator system, *Resources*, 4(3):692–712, 2015.

[4] Dornan, M. Renewable energy development in small island developing states of the Pacific. *Resources*, 4(3):490-506, 2015.

[5] Asif, M., and Muneer, T. Energy supply, its demand and security issues for developed and emerging economies. *Renewable and Sustainable Energy Reviews*, 11(7):1388-1413, 2007.

[6] Shafiee, S., and Topal, E. When will fossil fuel reserves be diminished?. *Energy Policy*, 37(1):181-189, 2009.

[7] Asmelash, E., and Gorini, R. International oil companies and the energy transition, International Renewable Energy Agency, Abu Dhabi, 2021, Accessed 12 October 2022. https://www.irena.org/publications/2021/Feb/Oil-companies-and-the-energy-transition.

[8] BP Statistical review of world energy, 2021, Accessed 12 October 2022. https://www.bp.com/content/dam/bp/business-sites/en/global/corporate/pdfs/energy-economics/statistical-review/bp-stats-review-2021-full-report.pdf

[9] Zhongming, Z., Linong, L., Xiaona, Y., Wangqiang, Z., and Wei, L. Global Energy Review 2021, Accessed 12 October 2022. https://www.iea.org/reports/global-energy-review-2021

[10] Tour, J. M., Kittrell, C. and Colvin, V. L. Green carbon as a bridge to renewable energy. *Nature Materials*, 9(11):871-874, 2010.

[11] Tollefson, J. Hydrogen vehicles: Fuel of the future. *Nature*, 464(7293):1262-1264, 2010.

[12] Ahmad, S., and Tahar, R. M. Selection of renewable energy sources for sustainable development of electricity generation system using analytic hierarchy process: A case of Malaysia. *Renewable Energy*, 63:458-466, 2014.

[13] Owusu, P. A., and Asumadu-Sarkodie, S. A review of renewable energy sources, sustainability issues and climate change mitigation. *Cogent Engineering*, 3:1167990, 2016.

[14] Yue, M., Lambert, H., Pahon, E., Roche, R., Jemei, S., and Hissel, D. Hydrogen energy systems: A critical review of technologies, applications, trends and challenges. *Renewable and Sustainable Energy Reviews*, 146:111180, 2021.

[15] Jackson, R. B., Friedlingstein, P., Le Quéré, C., Abernethy, S., Andrew, R. M., Canadell, J. G., and Peters, G. P. Global fossil carbon emissions rebound near pre-COVID-19 levels. *Environmental Research Letters*, 17(3):031001, 2022.

[16] Nayak, P. K., Mahesh, S., Snaith, H. J., and Cahen, D. Photovoltaic solar cell technologies: Analysing the state of the art. *Nature Reviews Materials*, 4(4):269-285, 2019.

[17] Wang, H. F., and Xu, Q. Materials design for rechargeable metal-air batteries. *Matter*, 1(3):565-595, 2019.

[18] Li, Y., and Lu, J. Metal–air batteries: Will they be the future electrochemical energy storage device of choice? *ACS Energy Letters*, 2(6):1370-1377, 2017.

[19] Patowary, S., Chetry, R., Goswami, C., Chutia, B., and Bharali, P. Oxygen reduction reaction catalysed by supported nanoparticles: Advancements and challenges. *ChemCatChem*, 14(7):e202101472, 2022.

[20] Yang, X., Roling, L. T., Vara, M., Elnabawy, A. O., Zhao, M., Hood, Z. D., and Xia, Y. Synthesis and characterization of Pt–Ag alloy nanocages with enhanced activity and durability toward oxygen reduction. *Nano Letters*, 16(10):6644-6649, 2016.

[21] Wang, Y., Chen, K. S., Mishler, J., Cho, S. C., and Adroher, X. C. A review of polymer electrolyte membrane fuel cells: Technology, applications, and needs on fundamental research. *Applied Energy*, 88(4): 981-1007, 2011.

[22] Ogbonnaya, C., Abeykoon, C., Nasser, A., and Turan, A. Unitized regenerative proton exchange membrane fuel cell system for renewable power and hydrogen generation: Modelling, simulation, and a case study. *Cleaner Engineering and Technology*, 4:100241, 2021.

[23] Ebrahimi, M., Kujawski, W., Fatyeyeva, K., and Kujawa, J. A review on ionic liquids-based membranes for middle and high temperature polymer electrolyte membrane fuel cells (PEM FCs). *International Journal of Molecular Sciences*, 22(11):5430, 2021.

[24] Sazali, N., Wan Salleh, W. N., Jamaludin, A. S., and Mhd Razali, M. N. New perspectives on fuel cell technology: A brief review. *Membranes*, 10(5):99, 2020.

[25] PEM Fuel Cells, Accessed 12 October 2022. https://physics.nist.gov/MajResFac/NIF/pemFuelCells.html

[26] Yang, Z., Coutinho, D., Feng, F., Ferraris, J. P., and Balkus Jr, K. Novel inorganic/organic hybrid electrolyte membranes. *Preprints of Papers- American Chemical Society, Division of Fuel Chemistry*, 49(2):599, 2004.

[27] Han, X., Li, X., White, J., Zhong, C., Deng, Y., Hu, W., and Ma, T. Metal–air batteries: from static to flow system. *Advanced Energy Materials*, 8(27): 1801396, 2018.

[28] Cheng, F., and Chen, J. Metal–air batteries: from oxygen reduction electrochemistry to cathode catalysts. *Chemical Society Reviews*, 41(6):2172-2192, 2012.

[29] Wang, Z. L., Xu, D., Xu, J. J., and Zhang, X. B. Oxygen electrocatalysts in metal–air batteries: from aqueous to nonaqueous electrolytes. *Chemical Society Reviews*, 43(22):7746-7786, 2014.

[30] Wang, C., Yu, Y., Niu, J., Liu, Y., Bridges, D., Liu, X., and Hu, A. Recent progress of metal–air batteries—a mini review. *Applied Sciences*, 9(14):2787, 2019.

[31] Dong, Q., and Wang, D. Catalysts in metal–air batteries. *MRS Communications*, 8(2):372-386, 2018.

[32] Li, L., Chang, Z. W., and Zhang, X. B. Recent progress on the development of metal-air batteries. *Advanced Sustainable Systems*, 1(10):1700036, 2017.

[33] Pan, J., Xu, Y. Y., Yang, H., Dong, Z., Liu, H., and Xia, B. Y. Advanced architectures and relatives of air electrodes in Zn–air batteries. *Advanced Science*, 5(4):1700691, 2018.

[34] Sinha, J., Lasher, S., and Yang, Y. Cost analyses of fuel cell stack/systems. *TIAX LLC 2010*, 2009, Accessed 12 October 2022. https://www.hydrogen.energy.gov/pdfs/progress09/v_a_3_sinha.pdf

[35] Nørskov, J. K., Rossmeisl, J., Logadottir, A., Lindqvist, L. R. K. J., Kitchin, J. R., Bligaard, T. and Jonsson, H. Origin of the overpotential for oxygen reduction

at a fuel-cell cathode. *The Journal of Physical Chemistry B*, 108(46):17886-17892, 2004.

[36] Keith, J. A., Jerkiewicz, G., and Jacob, T. Theoretical investigations of the oxygen reduction reaction on Pt (111). *ChemPhysChem*, 11(13):2779-2794, 2010.

[37] Yeager, E. Dioxygen electrocatalysis: Mechanisms in relation to catalyst structure. *Journal of Molecular Catalysis*, 38(1/2):5-26, 1986.

[38] Wakisaka, M., Suzuki, H., Mitsui, S., Uchida, H., and Watanabe, M. Increased oxygen coverage at Pt−Fe alloy cathode for the enhanced oxygen reduction reaction studied by EC−XPS. *The Journal of Physical Chemistry C*, 112(7): 2750-2755, 2008.

[39] Chen, W., Xiang, Q., Peng, T., Song, C., Shang, W., Deng, T., and Wu, J. Reconsidering the benchmarking evaluation of catalytic activity in oxygen reduction reaction. *Science*, 23:101532, 2020.

[40] Fabbri, E., and Schmidt, T. J. Oxygen evolution reaction—the enigma in water electrolysis. *ACS Catalysis*, 8(10):9765-9774, 2018.

[41] Fabbri, E., Habereder, A., Waltar, K., Kötz, R., and Schmidt, T. J. Developments and perspectives of oxide-based catalysts for the oxygen evolution reaction. *Catalysis Science & Technology*, 4(11):3800-3821, 2014.

[42] Suen, N. T., Hung, S. F., Quan, Q., Zhang, N., Xu, Y. J., and Chen, H. M. Electrocatalysis for the oxygen evolution reaction: Recent development and future perspectives. *Chemical Society Reviews*, 46(2):337-365, 2017.

[43] Tahir, M., Pan, L., Idrees, F., Zhang, X., Wang, L., Zou, J. J., and Wang, Z. L. Electrocatalytic oxygen evolution reaction for energy conversion and storage: A comprehensive review. *Nano Energy*, 37:136-157, 2017.

[44] Wang, J. X., Uribe, F. A., Springer, T. E., Zhang, J., and Adzic, R. R. Intrinsic kinetic equation for oxygen reduction reaction in acidic media: The double Tafel slope and fuel cell applications. *Faraday Discussions*, 140:347-362, 2009.

[45] Seh, Z. W., Kibsgaard, J., Dickens, C. F., Chorkendorff, I. B., Nørskov, J. K., and Jaramillo, T. F. Combining theory and experiment in electrocatalysis: Insights into materials design. *Science*, 355(6321): eaad4998, 2017.

[46] Xia, W., Mahmood, A., Liang, Z., Zou, R., and Guo, S. Earth-abundant nanomaterials for oxygen reduction. *Angewandte Chemie International Edition*, 55(8):2650-2676, 2016.

[47] Zeng, K., Zheng, X., Li, C., Yan, J., Tian, J. H., Jin, C., and Yang, R. Recent advances in non-noble bifunctional oxygen electrocatalysts toward large-scale production. *Advanced Functional Materials*, 30(27):2000503, 2020.

[48] Wang, Y., Su, H., He, Y., Li, L., Zhu, S., Shen, H. Xie, P., Fu, X., Zhou, G., Feng, C., and Zhao, D. Advanced electrocatalysts with single-metal-atom active sites. *Chemical Reviews*, 120(21):12217-12314, 2020.

[49] Goswami, C., Yamada, Y., Matus, E. V., Ismagilov, I. Z., Kerzhentsev, M., and Bharali, P. Elucidating the role of oxide–oxide/carbon interfaces of CuOx–CeO_2/C in boosting electrocatalytic performance. *Langmuir*, 36(49):15141-15152, 2020.

[50] Borah, B. J., Saikia, H., Goswami, C., Hazarika, K. K., Yamada, Y., and Bharali, P. Unique half embedded/exposed PdFeCu/c interfacial nanoalloy as high-performance electrocatalyst for oxygen reduction reaction. *ChemCatChem*, 11(15):3522-3529, 2019.

[51] Hazarika, K. K., Goswami, C., Saikia, H., Borah, B. J., and Bharali, P. Cubic Mn_2O_3 nanoparticles on carbon as bifunctional electrocatalyst for oxygen reduction and oxygen evolution reactions. *Molecular Catalysis*, 451:153-160, 2018.

[52] Liu, S., Sun, C., Chen, J., Xiao, J., and Luo, J. L. A high-performance Ruddlesden–Popper perovskite for bifunctional oxygen electrocatalysis. *ACS Catalysis*, 10(22):13437-13444, 2020.

[53] Xiao, M., Chen, Y., Zhu, J., Zhang, H., Zhao, X., Gao, L., Wang, X., Zhao, J., Ge, J., Jiang, Z., and Chen, S. Climbing the apex of the ORR volcano plot via binuclear site construction: Electronic and geometric engineering. *Journal of the American Chemical Society*, 141(44):17763-17770, 2019.

[54] Lu, X. F., Xia, B. Y., Zang, S. Q., & Lou, X. W. D. Metal-Organic Frameworks Based Electrocatalysts for the Oxygen Reduction Reaction. *Angewandte Chemie, International edition*, 59(12):4634-4650, 2020.

[55] Li, H., Chen, C., Yan, D., Wang, Y., Chen, R., Zou, Y., and Wang, S. Interfacial effects in supported catalysts for electrocatalysis. *Journal of Materials Chemistry A*, 7(41):23432-23450, 2019.

[56] Huang, X., Shen, T., Zhang, T., Qiu, H., Gu, X., Ali, Z., and Hou, Y. Efficient oxygen reduction catalysts of porous carbon nanostructures decorated with transition metal species. *Advanced Energy Materials*, 10(11):1900375, 2020.

[57] Hu, C., and Dai, L. Carbon-based metal-free catalysts for electrocatalysis beyond the ORR. *Angewandte Chemie International Edition*, 55(39):11736-11758, 2016.

[58] Nie, Y., Li, L., and Wei, Z. Recent advancements in Pt and Pt-free catalysts for oxygen reduction reaction. *Chemical Society Reviews*, 44(8):2168-2201, 2015.

[59] Shen, P. K., Wang, C. Y., Sun, X., and Zhang, J. *Electrochemical Energy: Advanced Materials and Technologies*. CRC press, 2018.

[60] Han, L., Dong, S., and Wang, E. Transition-metal (Co, Ni, and Fe)-based electrocatalysts for the water oxidation reaction. *Advanced Materials*, 28(42): 9266-9291, 2016.

[61] Gong, X., Li, A., Wu, J., Wang, J., Wang, C., and Wang, J. Graphene-cobalt based oxygen electrocatalysts. *Catalysis Today*, 358:184-195, 2020.

[62] Conway, B. E., and Salomon, M. Electrochemical reaction orders: Applications to the hydrogen-and oxygen-evolution reactions. *Electrochimica Acta*, 9(12): 1599-1615, 1964.

[63] MacDonald, J. J., and Conway, B. E. The role of surface films in the kinetics of oxygen evolution at Pd+ Au alloy electrodes. *Proceedings of the Royal Society of London. Series A. Mathematical and Physical Sciences*, 269(1338):419-440, 1962.

[64] Zhang, G., Li, Y., Xiao, X., Shan, Y., Bai, Y., Xue, H.G., Pang, H., Tian, Z. and Xu, Q. In situ anchoring polymetallic phosphide nanoparticles within porous prussian blue analogue nanocages for boosting oxygen evolution catalysis. *Nano Letters*, 21(7):3016-3025, 2021.

[65] Yoo, J. S., Rong, X., Liu, Y., and Kolpak, A. M. Role of lattice oxygen participation in understanding trends in the oxygen evolution reaction on perovskites. *ACS Catalysis*, 8(5):4628-4636, 2018.

[66] Chen, Z., Kronawitter, C. X., Yang, X., Yeh, Y. W., Yao, N., and Koel, B. E. The promoting effect of tetravalent cerium on the oxygen evolution activity of copper oxide catalysts. *Physical Chemistry Chemical Physics*, 19(47):31545-31552, 2017.

[67] Chou, S. C., Tso, K. C., Hsieh, Y. C., Sun, B. Y., Lee, J. F., and Wu, P. W. Facile synthesis of Co_3O_4@CoO@Co gradient core@ shell nanoparticles and their applications for oxygen evolution and reduction in alkaline electrolytes. *Materials*, 13(12):2703, 2020.

[68] Karmakar, A., and Srivastava, S. K. Transition-metal-substituted cobalt carbonate hydroxide nanostructures as electrocatalysts in alkaline oxygen evolution reaction. *ACS Applied Energy Materials*, 3(8):7335-7344, 2020.

[69] Zhang, S., Huang, B., Wang, L., Zhang, X., Zhu, H., Zhu, X., Li, J., Guo, S., and Wang, E. Boosted oxygen evolution reactivity via atomic iron doping in cobalt carbonate hydroxide hydrate. *ACS Applied Materials & Interfaces*, 12(36):40220-40228, 2020.

[70] Ramos-Garcés, M. V., and Colón, J. L. Preparation of zirconium phosphate nanomaterials and their applications as inorganic supports for the oxygen evolution reaction. *Nanomaterials*, *10*(5):822, 2020.

[71] Dresp, S., and Strasser, P. Non-noble metal oxides and their application as bifunctional catalyst in reversible fuel cells and rechargeable air batteries. *ChemCatChem*, 10(18):4162-4171, 2018.

[72] Chutia, B., Hussain, N., Puzari, P., Jampaiah, D., Bhargava, S. K., Matus, E. V., Ismagilov, I.Z., Kerzhentsev, M., and Bharali, P. Unraveling the role of CeO_2 in stabilization of multivalent Mn species on α-MnO_2/Mn_3O_4/CeO_2/C surface for enhanced electrocatalysis. *Energy & Fuels*, 35(13):10756-10769, 2021.

[73] Goswami, C., Hazarika, K. K., Yamada, Y., and Bharali, P. Nonprecious hybrid metal oxide for bifunctional oxygen electrodes: Endorsing the role of interfaces in electrocatalytic enhancement. *Energy & Fuels*, 35(16):13370-13381, 2021.

[74] Zhao, Y. M., Wang, F. F., Wei, P. J., Yu, G. Q., Cui, S. C., and Liu, J. G. Cobalt and iron oxides Co-supported on carbon nanotubes as an efficient bifunctional catalyst for enhanced electrocatalytic activity in oxygen reduction and oxygen evolution reactions. *ChemistrySelect*, 3(1):207-213, 2018.

[75] Cheng, F., Su, Y., Liang, J., Tao, Z., and Chen, J. MnO_2-based nanostructures as catalysts for electrochemical oxygen reduction in alkaline media. *Chemistry of Materials*, 22(3):898-905, 2010.

[76] Gorlin, Y., and Jaramillo, T. F. A bifunctional nonprecious metal catalyst for oxygen reduction and water oxidation. *Journal of the American Chemical Society*, 132(39):13612-13614, 2010.

[77] Chen, Y., Rui, K., Zhu, J., Dou, S. X., and Sun, W. Recent progress on nickel-based oxide/(oxy) hydroxide electrocatalysts for the oxygen evolution reaction. *Chemistry–A European Journal*, 25(3):703-713, 2019.

[78] Zhou, T., Xu, W., Zhang, N., Du, Z., Zhong, C., Yan, W., Ju, H., Chu, W., Jiang, H., Wu, C., and Xie, Y. Ultrathin cobalt oxide layers as electrocatalysts for high-performance flexible Zn–air batteries. *Advanced Materials*, 31(15):1807468, 2019.

[79] Han, X., He, G., He, Y., Zhang, J., Zheng, X., Li, L., Zhong, C., Hu, W., Deng, Y., and Ma, T.Y. Engineering catalytic active sites on cobalt oxide surface for enhanced oxygen electrocatalysis. *Advanced Energy Materials*, 8(10):1702222, 2018

[80] Li, Y., Zhou, Z., Cheng, G., Han, S., Zhou, J., Yuan, J., Sun, M., and Yu, L. Flower-like $NiCo_2O_4$–CN as efficient bifunctional electrocatalyst for Zn-Air battery. *Electrochimica Acta*, 341:135997, 2020.

[81] Rios, E. D. M. U. N. D. O., Gautier, J. L., Poillerat, G., and Chartier, P. Mixed valency spinel oxides of transition metals and electrocatalysis: Case of the $Mn_xCo_{3-x}O_4$ system. *Electrochimica Acta*, 44(8-9):1491-1497, 1998.

[82] Lee, H., Gwon, O., Lim, C., Kim, J., Galindev, O., and Kim, G. Advanced electrochemical properties of $PrBa_{0.5}Sr_{0.5}Co_{1.9}Ni_{0.1}O_{5+\delta}$ as a bifunctional catalyst for rechargeable zinc-air batteries. *ChemElectroChem*, 6(12):3154-3159, 2019.

[83] Bu, Y., Gwon, O., Nam, G., Jang, H., Kim, S., Zhong, Q., Cho, J., and Kim, G. A highly efficient and robust cation ordered perovskite oxide as a bifunctional catalyst for rechargeable zinc-air batteries. *ACS Nano*, 11(11):11594-11601, 2017.

[84] Liu, K., Huang, X., Wang, H., Li, F., Tang, Y., Li, J., and Shao, M. Co_3O_4–CeO_2/C as a highly active electrocatalyst for oxygen reduction reaction in Al–air batteries. *ACS Applied Materials & Interfaces*, 8(50):34422-34430, 2016.

[85] Zhang, Q., Han, W., Xu, Z., Li, Y., Chen, L., Bai, Z., Yang, L., and Wang, X. Hollow waxberry-like cobalt–nickel oxide/S, N-codoped carbon nanospheres as a trifunctional electrocatalyst for OER, ORR, and HER. *RSC Advances*, 10(46):27788-27793, 2020.

[86] Chen, Y. X., Chen, S. P., Zhou, Z. Y., Tian, N., Jiang, Y. X., Sun, S. G., Ding, Y., and Wang, Z.L. Tuning the shape and catalytic activity of Fe nanocrystals from rhombic dodecahedra and tetragonal bipyramids to cubes by electrochemistry. *Journal of the American Chemical Society*, 131(31):10860-10862, 2009.

[87] Zhang, X., Zhang, Y., Huang, H., Cai, J., Ding, K., and Lin, S. Electrochemical fabrication of shape-controlled Cu_2O with spheres, octahedrons and truncated octahedrons and their electrocatalysis for ORR. *New Journal of Chemistry*, *42*(1):458-464, 2018.

[88] Liu, H., Zhu, X., Li, M., Tang, Q., Sun, G., and Yang, W. Single crystal (Mn, Co)$_3O_4$ octahedra for highly efficient oxygen reduction reactions. *Electrochimica Acta*, 144:31-41, 2014.

[89] Ohno, H. Making nonmagnetic semiconductors ferromagnetic. *Science*, 281(5379):951-956, 1998.

[90] Smyth, D. M. The effects of dopants on the properties of metal oxides. *Solid State Ionics*, 129(1-4):5-12, 2000.

[91] Zhang, J., Lian, J., Jiang, Q., and Wang, G. Boosting the OER/ORR/HER activity of Ru-doped Ni/Co oxides heterostructure. *Chemical Engineering Journal*, 439:135634, 2022.

[92] Jia, Y., Jiang, K., Wang, H., and Yao, X. The role of defect sites in nanomaterials for electrocatalytic energy conversion. *Chem*, 5(6):1371-1397, 2019.

[93] Zhao, R., Li, Q., Jiang, X., Huang, S., Fu, G., and Lee, J. M. Interface engineering in transition metal-based heterostructures for oxygen electrocatalysis. *Materials Chemistry Frontiers*, 5(3):1033-1059, 2021.

[94] Paulus, U. A., Schmidt, T. J., Gasteiger, H. A., and Behm, R. J. Oxygen reduction on a high-surface area Pt/Vulcan carbon catalyst: A thin-film rotating ring-disk electrode study. *Journal of Electroanalytical Chemistry*, 495(2):134-145, 2001.

[95] Kuroda, S., Tobori, N., Sakuraba, M., and Sato, Y. Charge–discharge properties of a cathode prepared with ketjen black as the electro-conductive additive in lithium ion batteries. *Journal of Power Sources*, 119:924-928, 2003.

[96] Li, W., Wang, X., Chen, Z., Waje, M., and Yan, Y. Carbon nanotube film by filtration as cathode catalyst support for proton-exchange membrane fuel cell. *Langmuir*, 21(21):9386-9389, 2005.

[97] Shao, M., Chang, Q., Dodelet, J. P., and Chenitz, R. Recent advances in electrocatalysts for oxygen reduction reaction. *Chemical Reviews*, 116(6):3594-3657, 2016.

[98] Chen, L., Xu, X., Yang, W., and Jia, J. Recent advances in carbon-based electrocatalysts for oxygen reduction reaction. *Chinese Chemical Letters*, 31(3):626-634, 2020.

[99] Mukherjee, D. and Reddy, B. M. Noble metal-free CeO_2-based mixed oxides for CO and soot oxidation. *Catalysis Today*, 309:227-235, 2018.

[100] Saikia, H., Hazarika, K. K., Chutia, B., Choudhury, B., and Bharali, P. A simple chemical route toward high surface area CeO_2 nanoparticles displaying remarkable radical scavenging activity. *ChemistrySelect*, 2(11):3369-3375, 2017.

[101] Reddy, B. M., Bharali, P., Saikia, P., Park, S. E., van den Berg, M. W., Muhler, M., and Grünert, W. Structural characterization and catalytic activity of nanosized $Ce_xM_{1-x}O_2$ (M= Zr and Hf) mixed oxides. *The Journal of Physical Chemistry C*, 112(31):11729-11737, 2008.

[102] Jampaiah, D., Venkataswamy, P., Tur, K. M., Ippolito, S. J., Bhargava, S. K. and Reddy, B. M. Effect of MnO_x Loading on structural, surface, and catalytic properties of CeO_2-MnO_x mixed oxides prepared by sol-gel method. *Zeitschrift für anorganische und allgemeine Chemie*, 641(6):1141-1149, 2015.

[103] Jampaiah, D., Velisoju, V. K., Devaiah, D., Singh, M., Mayes, E. L., Coyle, V. E., Reddy, B.M., Bansal, V., and Bhargava, S.K. Flower-like Mn_3O_4/CeO_2 microspheres as an efficient catalyst for diesel soot and CO oxidation:

Synergistic effects for enhanced catalytic performance. *Applied Surface Science*, 473:209-221, 2019.

[104] Chen, J., Zhou, N., Wang, H., Peng, Z., Li, H., Tang, Y., and Liu, K. Synergistically enhanced oxygen reduction activity of MnO_x–CeO_2/Ketjenblack composites. *Chemical Communications*, 51(50):10123-10126, 2015.

[105] Masuda, T., Fukumitsu, H., Fugane, K., Togasaki, H., Matsumura, D., Tamura, K., Nishihata, Y., Yoshikawa, H., Kobayashi, K., Mori, T., and Uosaki, K. Role of cerium oxide in the enhancement of activity for the oxygen reduction reaction at Pt–CeO_x nanocomposite electrocatalyst-an in situ electrochemical X-ray absorption fine structure study. *The Journal of Physical Chemistry C*, 116(18):10098-10102, 2012.

[106] Yousaf, A. B., Imran, M., Uwitonze, N., Zeb, A., Zaidi, S. J., Ansari, T. M., Yasmeen, G., and Manzoor, S. Enhanced electrocatalytic performance of Pt_3Pd_1 alloys supported on CeO_2/C for methanol oxidation and oxygen reduction reactions. *The Journal of Physical Chemistry C*, 121(4):2069-2079, 2017.